Transition edge $YBa_2Cu_3O_{7-x}$ microbolometers for infrared staring arrays

M.C. Foote,[1] B.R. Johnson,[2] and B.D. Hunt[1]

[1] Center for Space Microelectronics Technology, Jet Propulsion Laboratory
California Institute of Technology, Pasadena, CA 91109

[2] Honeywell Technology Center, Honeywell, Inc.
Bloomington, MN 55420

ABSTRACT

High-temperature superconducting staring arrays are potentially important for both space and terrestrial applications which require the combination of high sensitivity over a broad wavelength range and relatively high temperature operation, in many such array applications sensitivity is more important than speed of response. Thus, it is desirable to design low-thermal-mass pixels that are thermally isolated from the substrate. To this end, Johnson, et al. [1,2] at Honeywell have fabricated meander lines of $YBa_2Cu_3O_{7-x}$ (YBCO) sandwiched between layers of silicon nitride on silicon substrates. The silicon was etched out from under each YBCO meander line to form low-thermal-mass, thermally isolated microbolometers. These 125 μm x 125 μm devices are estimated to have a noise equivalent power of 1.1x 10-12 $W/Hz^{1/2}$ near 5 Hz with a 5 μA bias (neglecting contact noise). A drawback of this original Honeywell design is that the YBCO is grown on an amorphous silicon nitride underlayer, which precludes the possibility of epitaxial YBCO growth. The YBCO therefore has a broad resistive transition, which limits the bolometer response, and the grain boundaries lead to excess noise. We discuss the potential performance improvement that could be achieved by using epitaxial YBCO films grown on epitaxial yttria-stabilized zirconia buffer layers on silicon. This analysis shows a significant signal to noise improvement at all frequencies in devices incorporating epitaxial YBCO films. Progress toward fabricating such devices is discussed.

1. INTRODUCTION

A potentially important application of high-temperature superconductors is sensing elements in microbolometers for infrared staring arrays. Such arrays will offer high sensitivity over a broad wavelength range and can be made on silicon substrates, taking advantage of the vast silicon technology base. NASA has a particular interest in long wavelength infrared detectors (10- 100 μm) for planetary space probes and for limb sounding of Earth's atmosphere from space. Above about 20μm, high-temperature superconducting microbolometers should easily outperform any existing detectors that operate in the same temperature range or higher. At shorter wavelengths, these devices have sensitivity high enough to compete favorably with (Hg,Cd)Te detectors, when considering the potentially much lower cost of the silicon-based technology used to fabricate the superconducting microbolometers. In addition, large format 2-D arrays of superconducting microbolometers on silicon should be easier to produce than arrays of (Hg,Cd)Te long wavelength detectors due to problems with (Hg,Cd)Te uniformity and thermal expansion mismatch with silicon readout circuitry.

Advanced technology for fabricating 2-D high density room temperature microbolometer arrays on silicon has been developed during the past ten years at Honeywell.[3] The Honeywell room temperature detector consists of a semiconducting thin film with a fairly sharp resistance versus temperature curve at room temperature ($(1/Ro)dRo/dT \approx 0.02$ K^{-1}, where R_o is the device resistance). This semiconducting film is sandwiched between two layers of silicon nitride (SN), forming a thin membrane supported by two SN legs over the silicon substrate. With this structure, the device heat capacity and thermal conductance to the substrate are extremely low, forming a very sensitive device with a useful time constant. A typical thermal response time is 10 ms, which allows the arrays to be operated at video frame rates (30 Hz). A prototype uncooled imaging camera has been demonstrated at Honeywell using a 340 x 240 pixel array. The measured noise equivalent temperature difference (NETD) for the 50 μm x 50 μm pixels is 40 mK for a 300 K object in the 8-12 μm spectral range using f/1.0 optics. Another imaging camera developed at Texas Instruments and based on pyroelectric detectors has shown similar performance at room temperature.[4]

A second effort at Honeywell has focused on improving the performance of the microbolometer arrays by substituting the high temperature superconductor YBCO for the semiconducting sensor element.[1,2] The YBCO in these devices is sandwiched between two layers of silicon nitride with thin yttria-stabilized zirconia (YSZ) layers to buffer the YBCO from the silicon nitride. These 125 μm x 125 μm devices are estimated to have a noise equivalent power (NEP) of 1.Ix10-12 $W/Hz^{1/2}$ near 5 Hz with a 5 μA bias (neglecting contact noise). A drawback of this design is that the YBCO is grown on an amorphous SN underlayer, which precludes the possibility of epitaxial YBCO growth, The YBCO, therefore, is polycrystalline with a broad resistive transition, which limits the bolometer responsivity, and the grain boundaries result in excess 1/' noise.

We are seeking to improve the Honeywell polycrystalline YBCO microbolometer by using epitaxial YBCO grown On epitaxial YSZ buffer layers on silicon. Such films can have very sharp resistive transitions, less than 1 h' in width,[5] and have been shown to have much lower excess film (l/f) noise than polycrystalline YBCO films.[6] Figure 1 shows a schematic diagram of the microbolometer design using epitaxial YBCO films. Here the YBCO is sandwiched between an underlayer of YSZ and a top layer of SN. The SN serves both as the primary membrane structural support and to protect the top side of the YBCO from the KOH etch used to remove the silicon from under the membrane.

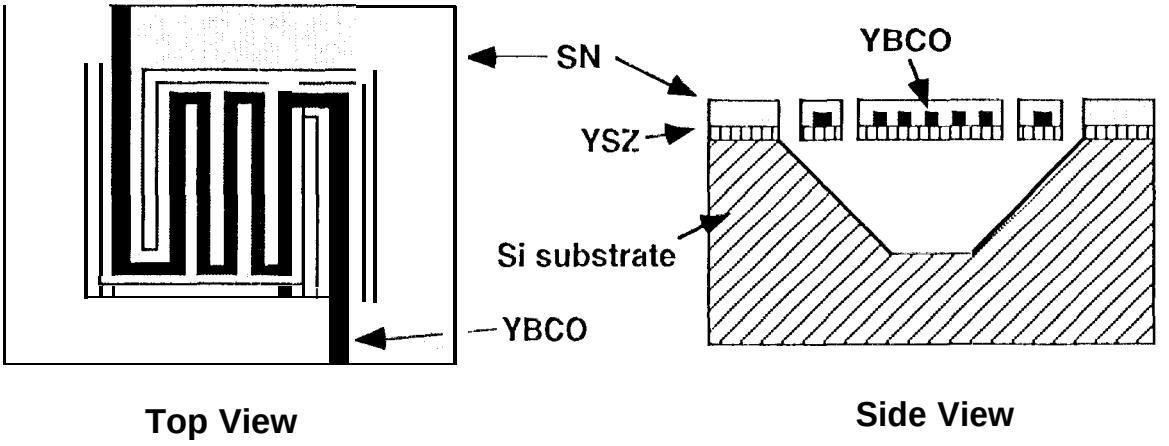

Fig. 1, Schematic diagram of YBCO microbolometer using epitaxial YBCO on an epitaxial YSZ buffer layer on a silicon substrate.

In this paper we first review the. performance of the original 1 loneywell polycrystalline YBCO microbolometers, including the contributions of the various noise sources. Then the potential performance improvement of microbolometers incorporating epitaxial YBCO films is calculated. Finally, the fabrication techniques for the epitaxial YBCO devices and the results to date are discussed.

2. DEVICE PERFORMANCE

Figure 2 shows estimated voltage noise contributions as a function of frequency for the Honeywell polycrystalline YBCO devices at a drive current of 5 μA. These values represent the best YBCO devices made at Honeywell using amorphous SN underlayers. The device noise was actually dominated by contact noise at the Au/YBCO electrical contacts, but we assume that low noise electrical contacts can be. produced, so will only discuss noise sources within the device. The drive current was chosen to be 5 μA in order to maximize the responsivity without causing excessive self heating of the microbolometer pixel. A constant drive current 1 reduces the effective thermal conductance G to the substrate. by $I^2(dR_o/dT)$ due to positive thermal feedback. The reduced thermal conductance results in slower thermal response. A drive current of 5 μA results in a reduction in effective thermal conductance of only 8%.

The 1/f noise. contribution shown in figure 2 is estimated from measurements on a heat sunk test structure with drive currents of 100 μA and 200 μA and at frequencies between 100 and 1000 Hz.[1] In this frequency range the excess film noise power varies as I/f, For this analysis it is assumed that this l/f dependence of the noise power is valid at all frequencies and that the noise power scales with the square of the drive current.

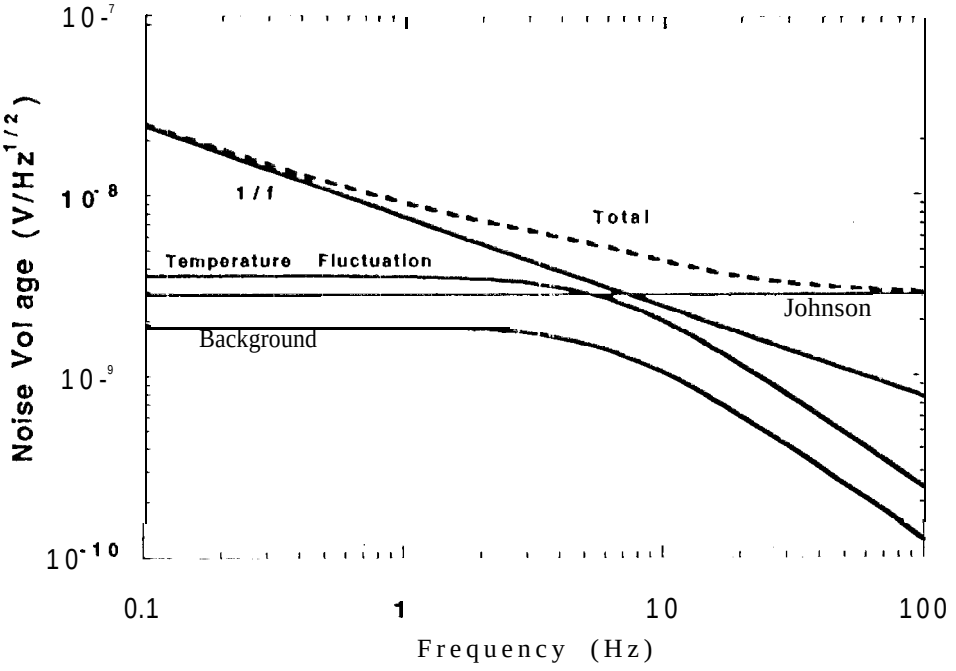

Fig. 2. Estimated voltage noise contributions and total noise voltage as a function of frequency for Honeywell polycrystalline YBCO microbolometers with a constant drive current of 5 μA.

The Johnson noise contribution is a calculated value using the measured resistance. of R_O= 2000 Ω and the formula

$$\frac{\Delta V_J}{\sqrt{B}} = \sqrt{4 k_B T_D R_0} \tag{1}$$

where k_B is the Boltzmann constant, B is the bandwidth, and T_D is the detector temperature of 73 K.

The temperature fluctuation noise and the background (photon) noise contributions are both due to pixel temperature fluctuations: the first due to thermal exchange by conduction to the substrate and the second due to radiative exchange with matter in the field of view. Because these noise contributions are thermal, their magnitude is proportional to the detector responsivity, which is defined as the voltage response per watt of incident power'. Temperature fluctuation noise, background noise, and responsivity all have the same frequency dependence, which rolls off with the thermal time constant $\tau = C/G = 24\ ms$, where C is the pixel heat capacity and G = 2 .0x 10-7 W/K is the measured thermal conductance to the substrate.. The temperature fluctuation noise in figure 2 is calculated from

$$\frac{\Delta V_{TF}}{\sqrt{B}} = \frac{2 k_B^{1/2} I R_0 \alpha T_D}{G^{1/2} (1 + 4\pi^2 f^2 \tau^2)^{1/2}} \tag{2}$$

where 1 is the drive current of 5 μA and f the measuring frequency. The temperature coefficient of resistance $\alpha = 0.30\ K^{-1}$ is a measure of the steepness of the pixel resistance versus temperature curve, and is defined by the value of $(1/Ro)dRo/dT$ at the transition midpoint. The background photon noise for a detector surrounded by a blackbody at uniform temperature T_B is given by[7]

$$\frac{\Delta V_{BG}}{\sqrt{B}} = \frac{I R_0 \alpha \left[8 A \eta \sigma k_B (T_D^5 + T_B^5)\right]^{1/2}}{G(1 + 4\pi^2 f^2 \tau^2)^{1/2}} \tag{3}$$

where A is the total detecting area, including both top and bottom surfaces. Each side of the pixel has an absorbing area 85 μm x 115 μm. The pixel absorptance is η=0.68 and σ is the Stefan-Boltzmann constant. We assume the background to be at 300 K. It is also assumed that the detector has cold shielding that covers the entire field of view except for one steradian, which is the solid angle subtended by the lens in a typic-al infrared optical system. Background noise is negligible from the shielded area, so equation 3 is reduced by $1/(4\pi)^{1/2}$. The total voltage noise shown in figure 2 is simply the square root of the sum of the squares of the individual voltage noise contributions.

The relationship between signal and noise can be expressed as the noise equivalent power (NEP), which is the incident photon power required to make an output voltage signal equal to the noise voltage. The NEP is simply the total voltage noise divided by the responsivity. The responsivity is given by

$$R = \frac{IR_0\alpha\eta\beta}{G(1+4\pi^2 f^2\tau^2)^{1/2}} \tag{4}$$

where β is the pixel fill factor. The Honeywell polycrystalline YBCO microbolometers have sensing elements that fill about 63% of the 125 μm x 125 μm etch pit area. Their responsivity was measured to be about 6500 V/W at S μA and $f = 1$ Hz. For these devices, the estimated NEP as a function of frequency is shown in Figure 3 (solid line). Near 5 Hz, the NEP is 1.1 XI O-] $^{2}W/Hz^{1/2}$. At lower frequencies the NEP increases because the responsivity remains fairly flat anti the $1/f$ noise increases. At frequencies above about 10 Hz, the responsivity rolls off as $1/f$ and the noise becomes dominated by a constant value of Johnson noise, so the NEP increases rapidly.

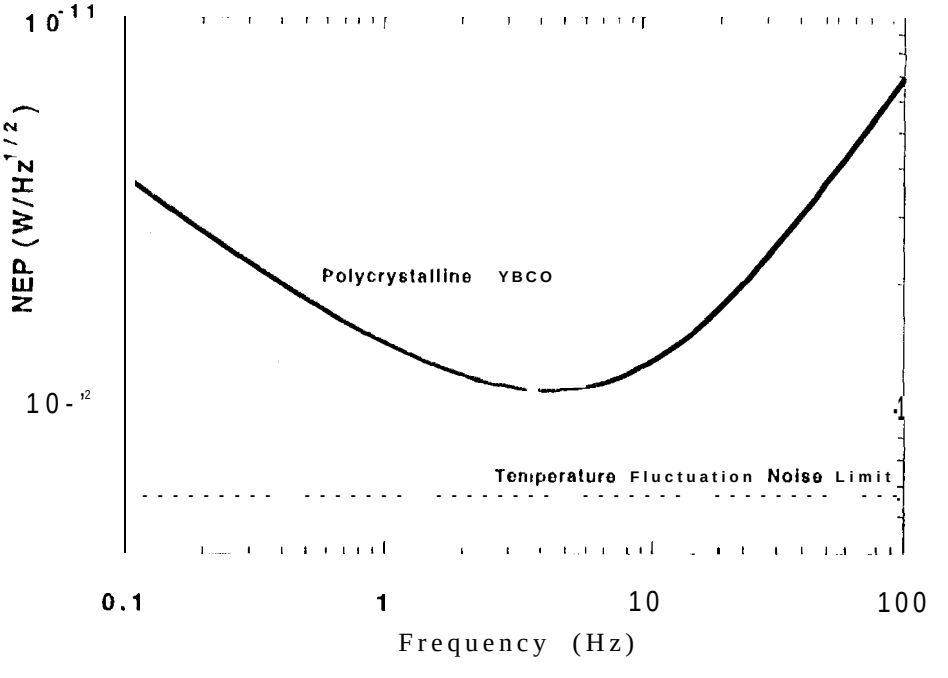

Fig. 3. Estimated NEP for Honeywell polycrystalline YBCO devices with a constant 5 μA drive current, and calculated temperature fluctuation noise limited NEP.

Ideally, one would like to reduce the relative importance of the Johnson noise, $1/f$ noise and temperature fluctuation noise until the dominant noise source is from background photon fluctuations. A more realistic goal for the present devices is to increase the temperature coefficient of resistance α in order to increase the responsivity. The result would be an increase. in the signal compared to the $1/f$ and Johnson noise. This increase in α increases the temperature fluctuation and

background noise proportionally, so with a large enough α the noise becomes dominated by temperature fluctuation noise, and the signal-to-noise ratio is temperature fluctuation noise limited. 'l'he temperature fluctuation limited NEP for the Honeywell polycrystalline YBCO devices is shown by the dashed line in figure 3. To increase the signal-to-noise ratio and decrease the temperature-fluctuation-limited value of NEP further requires modification of the pixel thermal properties, which is eventually limited by constraints on the thermal time constant and the mechanical design.

One can improve the performance of these original Honeywell YBCO microbolometers by substituting epitaxial YBCO for the polycrystalline material. Typical YBCO films made on epitaxial YSZ on silicon by pulsed laser deposition at JPI. have zero resistance values at 87-88 *K* and transition widths of 1 *K* or less. This narrow transition width results in values of temperature coefficient of resistance at the transition midpoint as high as α = 2.6 *K-l,* which is almost one order of magnitude larger than the value of 0.30 K^{-1} measured in (he Honeywell polycrystalline YBCO microbolometers. This improvement in α is partially offset by the fact that, with this sharper resistive transition, positive thermal feedback clue to the drive current is larger, so the drive current must be decreased. A constant drive current of 1.7 μA will cause the same reduction in effective thermal conductance for these epitaxial YBCO devices as 5 μA causes in the polycrystalline YBCO devices. Measurements of Verghese et al.[6] indicate that epitaxial YBCO films on silicon have at least one order of magnitude less I/'noise voltage than YBCO films on SN on silicon. We therefore assume that in devices with epitaxial YBCO, the $1/f$ noise is reduced by a factor of ten, plus an additional factor of three because of the lower drive current.

Thus, in this analysis of epitaxial YBCO device performance three assumptions are. made, 1) that a = 2.6 *K-],* with a corresponding reduction in drive current to 1.? μA, 2) that the $1/f$ noise voltage is reduced by a factor of thirty relative to the Honeywell polycrystalline YBCO films, and 3) that the operating temperature is 88 A' instead of the polycrystalline YBCO device operating temperature of 73 *h'*. Other device parameters are assumed to be the same for both the epitaxial and the polycrystalline YBCO devices. Given these assumptions, the contributions of the. various voltage noise sources for the epitaxial YBCO devices arc shown in figure 4. In comparison to the noise contributions in the polycrystalline YBCO devices, the temperature fluctuation and background noise have increased significantly, accompanied by a significant decrease in the 1/' noise. In combination, these two effects result in a total noise that is dominated by tempe rature fluctuation noise below about 20 Hz.

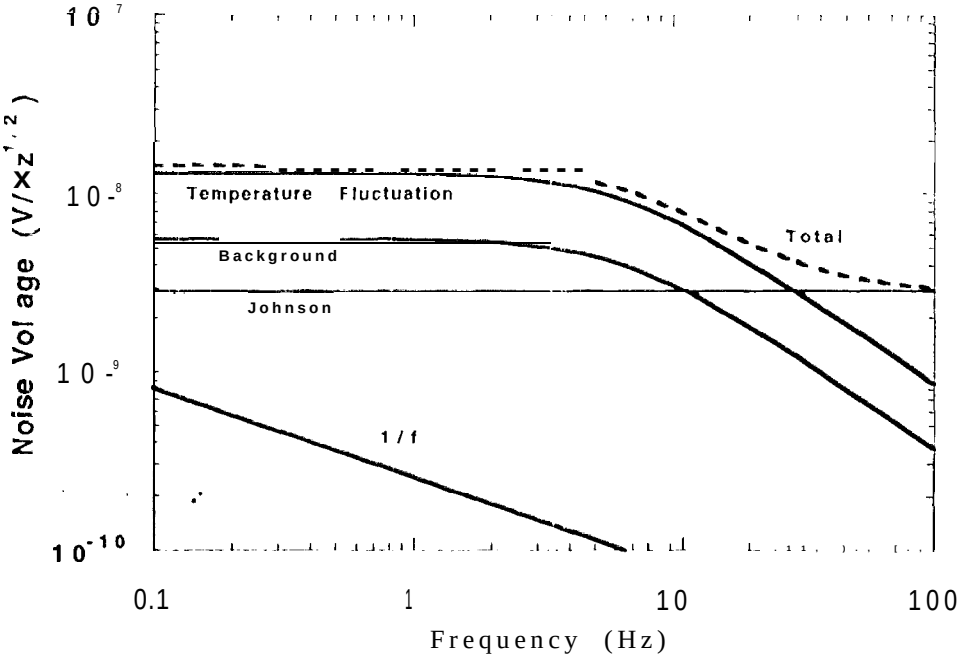

Fig. 4. Predicted voltage noise contributions and total noise voltage as a function of frequency for epitaxial YBCO microbolometers with a constant drive current of 1.7 μA.

Although the total noise in the epitaxial YBCO devices is larger at some frequencies than that in the polycrystalline YBCO devices, this effect is more than offset by an increase in responsivity. The Nil' for the two types of devices is **shown in figure. 5.** A significant reduction in NEP occurs for the epitaxial YBCO devices at all frequencies. Note that although tbe NEP for the. epitaxial YBCO devices is nearly temperature fluctuation noise limited below about 20 *Hz*, the increased operating temperature of 88 *K* results in a larger NEP than the temperature fluctuation limit for the polycrystalline devices shown in figure 3.

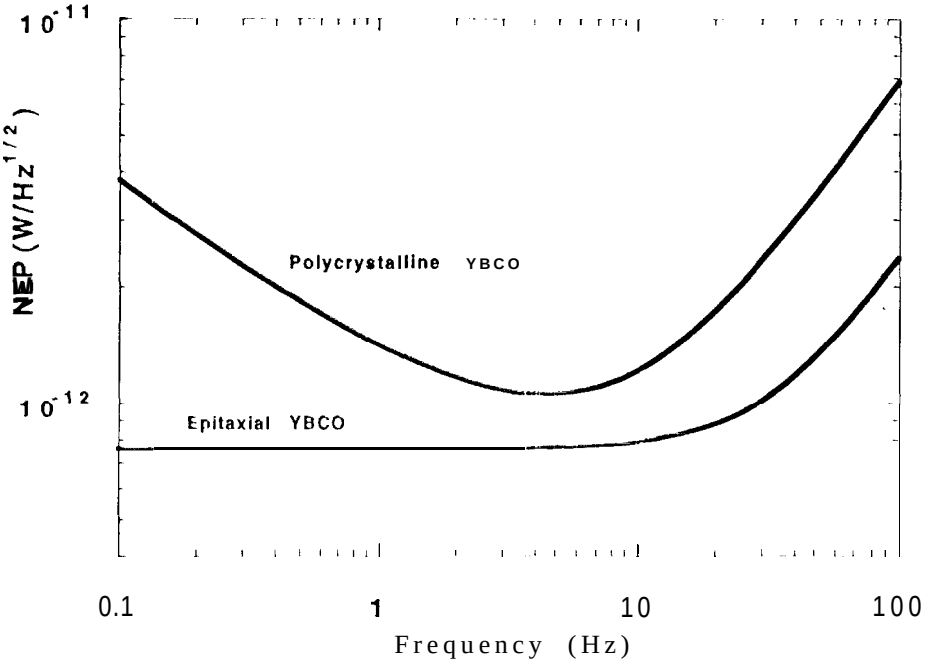

Fig. 5. Estimated NEP for Honeywell polycrystalline YBCO devices with a 5 μA drive current compared to predicted NEP for epitaxial YBCO devices with a 1.7 μA drive current.

The $1/f$ noise. contribution is dependent on sample size, with noise power typically scaling inversely with volume.[8] The devices described above arc 125 μm **x 125** μm **in** area, but for large format array applications, 50 μm pixels are more practical. If the devices are scaled down proportionally, the $1/f$ noise voltage should increase by a factor of roughly 125/50 = 2.5. Such an increase in $1/f$ noise should make little difference in signal to noise of the epitaxial YBCO devices, but would decrease the signal-to-noise ratio and increase the NEP of polycrystalline YBCO devices. This effect should increase the advantage gained by using epitaxial YBCO films. We note that this analysis is limited due to the uncertainty in extrapolating the measured $1/f$ noise contribution in the polycrystalline YBCO films to frequencies below 100 Hz.

7'0 summarize, we. have compared the performance obtained in the best Honeywell polycrystalline YBCO microbolometers to the predicted performance of similar devices using epitaxial YBCO films. The performance of devices made with the polycrystalline films was limited by $1/f$ and Johnson noise. Devices with epitaxial YBCO films are predicted to be nearly temperature fluctuation noise limited below about 20 *Hz* and to have a significantly lower noise equivalent power at all frequencies. Johnson and Kruse[2] have previously calculated the noise equivalent temperature difference of two-dimensional staring arrays using sensing films with properties similar to epitaxial YBCO. For 50 μm x 50 μm pixels having 10 *ms* thermal time constants fabricated from films having a temperature coefficient of resistance of 1.0 K^{-1} at 85 *K* and negligible I/f noise they predict a noise equivalent temperature difference as low as 2 *mK*. Their calculation assumed f/1.0 optics, a 30 *Hz* frame rate, and a 100 *kHz* system bandwidth, when viewing a 300 *K* blackbody.

3. FABRICATION

The fabrication process for microbolometers having epitaxial YBCO films involves first growing pulsed-laser deposited YBCO on HF-etched[9] silicon substrates with YSZ buffer layers using the method of Fork, et al.[5] A 1000 Å gold layer is sputter deposited in-situ on the YBCO to produce low-resistance electrical contacts. The Au/YBCO structure is then ion milled using a photoresist or metal mask to form the microbolometer meander and contact pad pattern. After an ion mill removal of the gold over the meander lines, a 1 μm layer of silicon nitride is deposited using an electron-cyclotron-resonance chemical vapor deposition process. A CF_4/O_2 plasma and ion milling are used to cut slits through the SN and YSZ around the meander pattern to allow the KOH etchant to attack the exposed silicon. Vias are etched through the SN to the contact pads using a CF_4/O_2 plasma, and additional gold is deposited over the contact pads to seal them from the etch. Finally, a hot KOH etch removes the silicon under the meander lines, forming isolated membranes connected to the substrate by thin legs.

4. RESULTS TO DATE

Figure 6 shows an electron micrograph of an 80 μm x 80 μm microbolometer pixel made with an epitaxial YBCO film. With the current process nearly 100% of the membranes survive the KOH etch mechanically intact. However, roughly half of the meander lines have regions where the YBCO is damaged by the KOH etchant. These damaged regions are easily visible in an optical microscope. Backside etch tests of YBCO/YSZ layers protected on the front by thick SN layers indicate that the YSZ is highly impermeable to the etching solution. We therefore conclude that most or all of the damaged regions are due to insufficient coverage of the YBCO by the SN cap layer. The coverage could be improved by using smoother YBCO films, reducing particles during processing, and modifying the SN deposition process. Nearly all of the membranes are flat and mechanically intact, indicating that stress is not a problem in these microstructures.

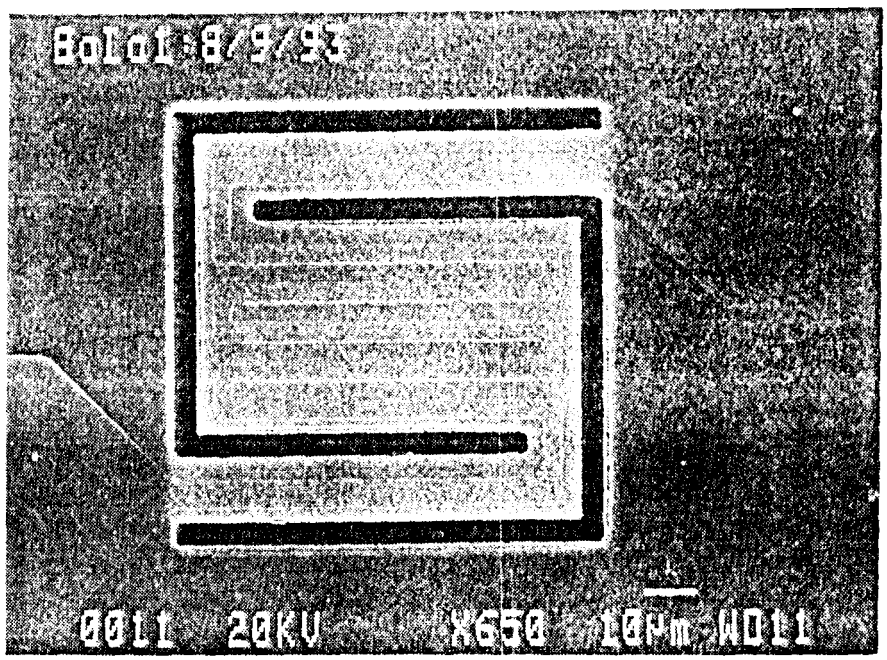

Fig. 6. Electron micrograph of an 80 µm x 80 µm microbolometer pixel made with an epitaxial YBCO film.

Microbolometers made to date using the epitaxial YBCO process have performed poorly due to degradation of the YBCO films during processing. Some previous reports[10,11] have indicated that epitaxial YBCO on silicon is very sensitive to traditional post-de position patterning. However, we have successfully patterned YBCO microbridges on silicon using photolithography and ion milling. These microbridges displayed transition temperatures between 85 and

90 K and critical current densities as high as 10^6 A/cm^2 at 77 K and 107 A/cm^2 at 4.2 K. Films of this quality should be adequate for microbolometer applications. We therefore believe that refine.]llents in the microbolometer processing will result in improved device performance.

5. CONCLUSIONS

Microbolometers using polycrystalline YBCO films have previously been fabricated at Honeywell.[1,2] These devices, which have a thermal time constant of 24 ms, have an estimated noise equivalent power of 1.1×10^{-12} $W/Hz^{1/2}$ near 5 Hz, which is within a factor of two of the temperature fluctuation limit for this structure. We have shown that significant improvements in NEP at all frequencies can be obtained by using superconducting films with sharper resistive transitions and lower $1/f$ noise, such as epitaxial YBCO grown on epitaxial YSZ on silicon. These devices, incorporated into staring arrays, will find applications where high sensitivity over a broad wavelength range and relatively high temperature operation is required.

6. ACKNOWLEDGMENTS

'l'he research described in this paper was performed by the Center for Space Microelectronics Technology, Jet Propulsion Laboratory, California Institute of Technology and by the Honeywell l'ethnology Center, and was jointly sponsored by the National Aeronautics and Space Administration, Office of Advanced Concepts and Technology, and by the Ballistic Missile Defense organization, Innovative Science and Technology Office.

7. REFERENCES

1. B.R. Johnson, 1'. Ohnstein, C.J.Han, R. Higashi, P.W. Kruse, R.A. Wood, H. Marsh, and S.B . Dunham, "$YBa_2Cu_3O_{7-x}$ superconductor microbolometer arrays fabricated by silicon micromachining", IEEE Trans. Appl. Supercond. **3**, pp. 2856-2.859 (1993).
2. B.R. Johnson and P.W. Kruse, "Silicon Microstructure Superconducting Microbolometer Infrared Arrays", Proc. SPIE Infrared Technology XIX, vol. 2020, pp. 2-7 (1993),
3. R.A. Wood, "Uncooled thermal imaging with monolithic silicon focal planes", proc. SPIE Infrared Technology Xl X, vol. 2020, pi). 322-329 (1993).
4. Charles Hanson, "Uncooled thermal imaging at Texas Instruments", proc. SPIE Infrared Technology XIX, vol. 2020, pp. 330-339 (1993).
5. D.K. Fork, D.B. Fenner, R.W. Barton, Julia M. Phillips, G.A N. Connell, J.B. Boyce ant] 'l'. II. Geballe, "High critical currents in strained epitaxial $YBa_2Cu_3O_{7-\delta}$ on Sin, Appl. Phys. Lett. 57, pp. 1] 61- 1163 (1990).
6. S. Verghese, P.L. Richards, K. Char, D.K. Fork and T.H. Geballe, "Feasibility of infrared imaging arrays using high-T_c superconducting bolometers", J. Appl. Phys. 71, pp. 2491-2498 (1992).
7. P.W. Kruse, L.D. McGlauchlin, and R. Il. McQuistan, "Elements of Infrared l'ethnology: generation, transmission, and detection", pp. 351-356, John Wiley & Sons, New York (1 962).
8. F.N. Hooge and A.M.H. Hoppenbrouwers, " 1/' Noise in Continuous Thin Gold Films", Physics vol. 45, p. 386-392 (1969).
9. F.J. Grunthaner and P.J. Grunthaner, "Chemical and Electronic Structure of the SiO_2/Si lntcr-face", Mater. Sci. Rep. **1**, pp. 65-160 (1986).
10. C.A. Copetti, J. Schubert, W. Zander, 11. Soltner, U. Poppe, and Ch. Buchal, "Aging of superconducting $Y_1Ba_2Cu_3O_{7-x}$ structures on silicon", J. Appl. Phys. 73, pp. 1339-1342 (1993).
11. R. One, private communication.